Full energy peak efficiency calibration of HPGe detector for point and extended sources using Monte Carlo code

**Chhavi Agarwal · Sanhita Chaudhury ·
A. Goswami · M. Gathibandhe**

Abstract Monte Carlo simulation is important to get efficiencies for cases where the experimental efficiencies are difficult to get such as for samples with nonstandard geometries and for large samples. In this paper, efficiency of the HPGe detector, routinely used in our lab for a variety of samples, has been computed for point source geometry and its parameters has been optimized to match MCNP and experimental efficiencies within 5% at different sample to detector distances. This optimized geometry was then validated by efficiency transfer to other geometries.

Keywords Full energy peak efficiency · Monte Carlo simulation · Detector geometry optimization

Introduction

Efficiency calibration of a gamma ray detector is carried out using a set of standards emitting gamma rays over the energy range of 50–1500 keV. Full energy peak (FEP) efficiency calibration is usually done using the mono-energetic gamma ray sources e.g. ^{241}Am, ^{109}Cd, ^{57}Co, ^{203}Hg, ^{51}Cr, ^{137}Cs and ^{65}Zn. The availability of mono-energetic primary standards is a constraint. Moreover, some of these sources are not very long lived e.g. ^{203}Hg ($t_{1/2}$-46.6 d), ^{51}Cr ($t_{1/2}$-27.7 d), so they need to be replaced periodically. Multi-gamma ray sources like ^{152}Eu and

C. Agarwal · S. Chaudhury · A. Goswami (✉)
Radiochemistry Division, Bhabha Atomic Research Centre,
Mumbai 400085, India
e-mail: agoswami@barc.gov.in

M. Gathibandhe
Reactor Projects Division, Bhabha Atomic Research Centre,
Mumbai 400085, India

^{133}Ba are often preferred for efficiency calibration as they cover a wide energy range and are longer lived. These sources emit gamma rays in cascade and for close sample to detector distances, there may be substantial coincidence summing leading to inaccuracy in efficiency calibration. Therefore, standard multi-gamma sources cannot be used for the gamma spectrometric analysis of low level samples where there is a need to count the samples as close as possible to the detector.

These difficulties can be circumvented by using Monte Carlo simulation for FEP efficiency. It is a powerful tool to simulate the detector response and is applicable to a variety of matrices and source geometries [1–4]. These codes are particularly useful to get efficiency for cases where experimental determination is impossible or difficult such as samples of non-standard geometry and for large sized samples e.g. environmental samples [5] and waste drums where standards are not easily available. Thus the simulation codes have been increasingly used for efficiency calibration. Also, these simulation methods are decay scheme independent and are consequently free of any coincidence summing and can be used at closest sample to detector distance where multi-gamma ray sources cannot be used. Additionally, these simulation codes can be used to get total efficiency required for coincidence summing correction. However, as reported in the literature, there is often a mismatch between the simulated and experimental efficiencies. This is due to the sensitivity of the Monte Carlo calculations to the detector geometry specifications. The dimensions provided by the manufacturer correspond to the time of assembly of the detection system at room temperature. But there can be changes in the mechanical support of the crystal due to contractions at low temperature leading to changes in the detector configuration [6]. Also, there can be uncertainty in the parameters e.g. dead

layer thickness, detector end cap to Ge crystal distance etc. There are reports in literature in which the physical characteristics of the detector have been measured experimentally to minimize these uncertainties [7–10]. The length of the sensitive region of the detector has been determined by scanning the detector along its axis and accuracy less than 1% has been achieved between experimental and calculated efficiency [7, 8]. The shape of the detector crystal and its position in the housing has been measured by gamma or X-ray radiography [9, 10]. The average dead layer thickness is generally measured by measuring the attenuation of a collimated photon beam. The average dead layer thickness on front face and on the cylindrical side of the crystal has been measured by using the [241]Am source [10]. It has been observed that there can be increase in dead layer thickness from 0.35 mm to 1.16 mm after 9 years of operating time [11].

The effect of different detector parameters on the FEP efficiency has been studied in the literature [12, 13]. Detector efficiency has been observed to vary significantly with crystal diameter and its position [12]. It has been observed that it is the detector overall volume and not the detector diameter or length that has a major effect on the FEP efficiency [13]. The influence of dead layer thickness on the detector efficiency response has been studied [4]. It has been observed that increase of dead layer leads to the decrease in the efficiency, not only due to attenuation of gamma rays in the dead layer but also due to the reduction of the active volume of the detector.

Due to the uncertainty in the detector parameters, which may result in uncertainty in efficiency calculation by Monte Carlo method, the general approach has evolved whereby the different detector parameters are optimized to reproduce the experimental point source efficiencies as a function of energy. Subsequently, efficiency for other geometries can be obtained accurately using the optimized parameters. There are other studies in literature where the detector geometry has been optimized by adjusting the detector parameters. Crystal dimensions such as the crystal diameter, length and crystal front dead layer thickness has been adjusted and attained results with a relative deviation within 5–10% [14–16]. Tzika et al. [17] optimized the detector geometry by changing the dead layer thickness and could get an overall agreement of 10%. Karamanis et al. [18] also increased Ge–Al distance by 8 mm and the entrance Li dead layer by 600 μm to get results within 5%. In EUROMET exercise [19], it was concluded that most of the simulation codes can be used for routine measurements where uncertainties of 5–10% in efficiencies are acceptable. There is literature where much better accuracy (<2%) has been obtained by optimizing the detector geometry [7, 8, 20]. The objective of this work was to optimize the detector parameters using experimental efficiencies for standard geometries such as point sources. The optimized detector parameters have been used for efficiency transfer to other geometries. Results are discussed in the light of existing observations in the literature.

Experimental

The detector used in the present work is a closed end coaxial p-type DSG HPGe detector. The detector has a 20% relative efficiency and a resolution of 2.1 keV for the ^{60}Co gamma ray at 1332 keV and is used for routine gamma spectrometric analysis in our lab. The schematic diagram of the detector geometry as specified by the manufacturer is shown in Fig. 1. The detector was first calibrated for its efficiency by counting point sources of standard [133]Ba and [152]Eu at 21.7 cm from the detector end cap. Such a large distance was chosen for efficiency calibration with these multi gamma sources so as to avoid any uncertainty in the efficiency curve due to coincidence summing. The counting of the samples was done for a sufficiently long time so as to keep statistical uncertainty less than a percent. All the spectra were analyzed by PHAST software [21]. The Eu–Ba efficiencies were fitted into a fourth order log–log polynomial curve by non linear least square fitting. These efficiencies were then used to calibrate point sources of [109]Cd, [57]Co, [203]Hg, ^{51}Cr, ^{137}Cs and [65]Zn procured from Board of Radiation and Isotope Technology, Mumbai. For calibration, these sources were also counted at $d = 21.7$ cm. The mono-energetic sources were then used to determine FEP efficiencies (ε_γ) at closer distances ($d = 1.7$ and 12.6 cm) by using the experimentally determined disintegration rate (dps) given by:

$$\varepsilon_\gamma = \frac{cps}{I_\gamma x \, dps} \tag{1}$$
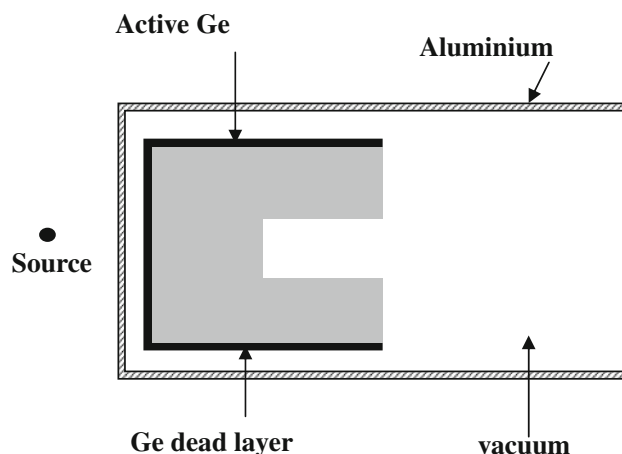
Fig. 1 Schematic diagram of the detector geometry supplied by manufacturer

where cps is the count rate at the energy of interest and I_γ is the gamma ray emission probabilities taken from Table of Isotopes [22]. The count rates were corrected for the background peak counts in all the cases.

Similarly, 5 ml sources of ^{109}Cd, ^{57}Co, ^{203}Hg, ^{137}Cs and ^{65}Zn were calibrated using standard 5 ml sources of ^{152}Eu and ^{133}Ba in same HPGe detector at $d = 10.3$ cm. These sources were then used to obtain efficiencies at $d = 2.0$ cm. Also, 100 ml standard source of ^{152}Eu taken in a glass bottle was counted in the same HPGe detector at $d = 19.8$ cm and FEP efficiencies were determined.

Monte Carlo simulation

In this work, the version MCNP4c [23] was used to simulate the HPGe detector response. This code tracks the particle from its origin point to the point of its complete absorption. All primary as well as secondary interactions are taken into account. The efficiency was obtained with F8 tally which is a pulse height tally. Mode P was used. The description of the detector geometry was given in detail in the cell and surface cards of the MCNP input file. The detector housing including the absorbing materials (aluminum end cap, germanium dead layer), were all included in the geometry. In each run $\sim 10^8$ particles were sampled to reduce statistical uncertainties.

Results and discussion

Initial MCNP simulations were performed for point source geometry with the dimensions of the detector obtained from manufacturer as given in the second column of Table 1. The MCNP simulated and experimental values of the FEP efficiencies are shown in Fig. 2. The error on experimental efficiencies is also shown in the figure and is obtained by propagating error on peak areas, abundances and efficiency fitting error. The error bars are of the size of the symbol.

At all sample to detector distances ($d = 1.7$, 12.6 and 21.7 cm), the MCNP efficiencies were found to be higher than the experimental values indicating the inadequacy of the manufacturer supplied detector dimensions. Similar observations have also been made in literature [7, 10, 12, 24]. A more detailed comparison of the MCNP and experimental efficiencies at $d = 1.7$, 12.6 and 21.7 cm has been given in Table 2. At a particular distance, the ratios of MCNP to experimental efficiencies were observed to be within 2–4% over the energy range of 88–1115 keV. But, these ratios were found to vary strongly from one distance to other with the MCNP to experimental ratio being higher for the closer distance. It can be seen from the table that the

Table 1 Detector parameters provided by manufacturer and optimized by MCNP simulation

Description	Nominal value (mm)	Optimized value (mm)
Crystal radius	24.55	23.65
Crystal length	49.9	49.9
Front Ge dead layer thickness	0.6	0.7
Side Ge dead layer thickness	0.6	0.6
Inner hole radius	4.25	4.25
Inner hole depth	38.4	38.4
Al end cap thickness	0.7	0.7
Al end cap to crystal distance	3	9
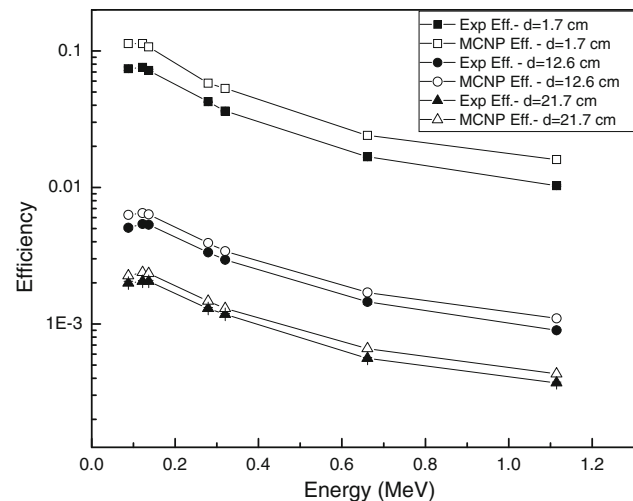
Fig. 2 Experimental and MCNP simulated FEP efficiency for point source geometry using the manufacturer supplied detector geometry at three sample to detector distances, $d = 1.7$, 12.6 and 21.7 cm

average MCNP to experimental ratio at $d = 21.7$ cm is 1.14 while it increases to 1.20 at $d = 12.6$ cm and to 1.46 at $d = 1.7$ cm. This indicates that the detector parameters have to be adjusted such that the constancy of efficiency over the energy range is not disturbed but the strong dependency on the sample to detector distance is removed. There are a number of geometrical parameters which can be uncertain like detector crystal radius, its length, inner hole radius and length, dead layer thickness, Al end cap thickness, the Al end cap to detector crystal distance. The effect of systematic change in these parameters on the FEP efficiency is discussed in the following.

Detector crystal geometry

Since crystal dimensions have been reported to have major effect on the detector efficiency, the radius of the detector

Table 2 The comparison of experimental and MCNP efficiencies at three sample to detector distances, $d = 1.7, 12.6$ and 21.7 cm

Energy (MeV)	$d = 1.7$ cm			$d = 12.6$ cm			$d = 21.7$ cm		
	MCNP eff	Exp eff	MCNP/exp	MCNP eff	Exp eff	MCNP/exp	MCNP eff	Exp eff	MCNP/exp
0.088	0.1132	0.0741	1.53	0.0063	0.0051	1.24	0.0023	0.0020	1.14
0.1221	0.1126	0.0757	1.49	0.0065	0.0054	1.20	0.0024	0.0020	1.16
0.1365	0.1073	0.0720	1.49	0.0064	0.0053	1.19	0.0023	0.0020	1.14
0.2792	0.0579	0.0424	1.36	0.0039	0.0033	1.17	0.0015	0.0013	1.13
0.32	0.0525	0.0363	1.44	0.0034	0.0030	1.16	0.0013	0.0012	1.11
0.661	0.0238	0.0168	1.41	0.0017	0.0015	1.17	0.0007	0.0006	1.17
1.115	0.0155	0.0103	1.50	0.0011	0.0009	1.22	0.0004	0.0004	1.15
		Avg.	1.46		Avg.	1.20		Avg.	1.14
		SD	0.06		SD	0.03		SD	0.02
		% RSD	3.92		% RSD	2.52		% RSD	1.90

The detector geometry used has been provided by the manufacturer

was reduced in steps of 1 mm and detector efficiency was computed by MCNP at $d = 1.7$ and 21.7 cm. Table 3 gives the comparison of FEP experimental and MCNP efficiency results. The average efficiency ratio has reduced from 1.46 to 1.36 at 1.7 cm and from 1.14 to 1.03 at $d = 21.7$ cm. The detector radius was further reduced by 1 mm, to see if the ratio further reduces and approaches unity. As given in

Table 3, although at $d = 1.7$ cm, the ratio has reduced to 1.16 but it became less than 1 at $d = 21.7$ cm. Thus, it can be concluded that the reduction in crystal radius by 1 mm can reproduce the experimental efficiency at long distance, but at shorter distance ($d = 1.7$ cm), the discrepancy still exists. Since the MCNP to experimental ratio should be close to unity at all sample to detector distance, variation of

Table 3 The ratio of MCNP and experimental efficiencies at two sample to detector distances, $d = 1.7$ and 21.7 cm

The MCNP efficiencies are computed by changing some detector crystal parameters to see its effect on the detector efficiency

Energy (MeV)	Crystal radius reduced by 1 mm MCNP/exp	Crystal radius reduced by 2 mm MCNP/exp	Crystal length reduced by 4.9 mm MCNP/exp	Inner hole radius increased by 5.75 mm MCNP/exp	Dead layer thickness increased by 0.4 mm MCNP/exp
$d = 1.7$ cm					
0.088	1.46	1.31	1.53	1.53	1.29
0.1221	1.41	1.25	1.49	1.44	1.37
0.1365	1.41	1.24	1.49	1.40	1.40
0.2792	1.27	1.08	1.35	0.95	1.33
0.32	1.34	1.13	1.42	1.33	1.41
0.661	1.29	1.05	1.36	1.22	1.39
1.115	1.36	1.09	1.43	1.26	1.48
Avg.	1.36	1.16	1.44	1.31	1.38
SD	0.07	0.10	0.07	0.19	0.06
% RSD	5.04	8.58	4.69	14.36	4.37
$d = 21.7$ cm					
0.088	1.05	0.88	1.14	1.13	0.99
0.1221	1.07	0.89	1.16	1.14	1.09
0.1365	1.04	0.88	1.13	1.11	1.08
0.2792	1.03	0.84	1.10	1.02	1.11
0.32	1.00	0.81	1.07	0.97	1.08
0.661	1.06	0.83	1.11	0.97	1.17
1.115	1.02	0.79	1.06	0.91	1.13
Avg.	1.04	0.85	1.11	1.04	1.09
SD	0.02	0.04	0.04	0.09	0.06
% RSD	2.26	4.48	3.22	8.72	5.06

crystal radius alone is not sufficient to match MCNP and experimental efficiency.

Since the crystal length can also have appreciable effect on efficiency, as a next step, it was reduced by 4.9 mm keeping the inner hole length constant, and as given in Table 3, the average MCNP to experimental ratio at both the distances decreased by about 2–3% only even after a reduction of detector length by 10%. Since the value of length quoted by the manufacturer cannot be erroneous by more than 10%, this parameter was not further changed and its original value was restored. The increment in inner hole radius to 5.75 mm and thereby reduction in the overall detector volume, as given in Table 3, introduced energy dependence which was earlier not present with the manufacturer supplied detector geometry. This was expected as the lower energy gamma rays will be absorbed in a small detector length and so will not be affected by increasing the inner hole radius but some part of the high energy gammas will escape due to increase in the inner hole radius. Therefore, in our case, this is not the parameter to be changed. The detector efficiency also depends upon the dead layer thickness, as low energy photons may be highly attenuated in it. The influence of dead layer thickness on the detector efficiency was seen by increasing the dead layer thickness by 0.4 mm. There was a reduction of only 4–5% in the MCNP to experimental efficiency ratios as

given in Table 3 after an increase in dead layer thickness by 67%. From this, it was concluded that, in our case the detector crystal parameters are not the one responsible for such a high efficiency ratio of 1.46 at $d = 1.7$ cm.

Detector end cap thickness and end cap to crystal distance

Since the effect of increasing the thickness of Al end cap will be similar and less in magnitude to increasing the Ge dead layer thickness, the Al thickness was not changed. The distance between the Al end cap and detector crystal (d_{alc}) was increased by 3 mm and MCNP efficiencies were computed at $d = 1.7$ and 21.7 cm. Table 4 gives the ratios of MCNP and experimental efficiency values. The MCNP efficiencies at 1.7 cm decreased by about 13% while the efficiencies at $d = 21.7$ cm reduced by only 2%. Since in our case, there is distance dependence in the MCNP to experimental ratio with the ratio being higher at closer distance, the Al end cap to crystal distance may be the cause of discrepancy between MCNP and experimental efficiency values. This is in accordance with Hardy et al. [8] who observed an uncertainty of $\sim 36\%$ in the Al end cap to crystal distance. The d_{alc} was then systematically changed and the results are presented in Table 4. When the

Table 4 The comparison of experimental and MCNP efficiencies at two sample to detector distances, $d = 1.7$ and 21.7 cm

Energy (MeV)	$d_{alc} = 3$ mm MCNP/exp	$d_{alc} = 6$ mm MCNP/exp	$d_{alc} = 8$ mm MCNP/exp	$d_{alc} = 8.5$ mm MCNP/exp	$d_{alc} = 9$ mm MCNP/exp	$d_{alc} = 10$ mm MCNP/exp
$d = 1.7$ cm						
0.088	1.53	1.32	1.21	1.18	1.15	1.10
0.1221	1.49	1.28	1.17	1.14	1.11	1.07
0.1365	1.49	1.29	1.17	1.14	1.12	1.07
0.2792	1.36	1.18	1.08	1.06	1.03	0.99
0.32	1.44	1.25	1.14	1.11	1.09	1.04
0.661	1.41	1.22	1.12	1.10	1.07	1.03
1.115	1.50	1.30	1.19	1.16	1.14	1.09
Avg.	1.46	1.26	1.15	1.13	1.10	1.05
SD	0.06	0.05	0.04	0.04	0.04	0.04
% RSD	3.92	3.86	3.77	3.76	3.78	3.71
$d = 21.7$ cm						
0.088	1.14	1.11	1.09	1.08	1.08	1.07
0.1221	1.16	1.13	1.11	1.11	1.10	1.10
0.1365	1.14	1.12	1.10	1.09	1.09	1.07
0.2792	1.13	1.11	1.09	1.09	1.08	1.07
0.32	1.11	1.08	1.06	1.05	1.05	1.04
0.661	1.17	1.15	1.13	1.13	1.12	1.13
1.115	1.15	1.12	1.10	1.10	1.10	1.09
Avg.	1.14	1.12	1.10	1.09	1.09	1.08
SD	0.02	0.02	0.02	0.02	0.02	0.03
% RSD	1.90	2.02	2.02	2.03	2.02	2.48

The MCNP efficiencies are computed by changing the Al end cap to detector crystal distance (d_{alc}) to see its effect on the detector efficiency

Al end cap to crystal distance is kept as 8 mm, the ratio of efficiencies was further decreased, but still a difference between the efficiency ratios at $d = 1.7$ and 21.7 cm can be seen. The principle of efficiency transfer says that this difference should not exist, so the Al end cap to crystal distance was further incremented in steps to 1 mm. The results are given in Table 4. It can be seen that as the Al end cap to crystal distance is increased, the ratios of MCNP to experimental efficiencies at $d = 1.7$ and 21.7 cm come closer and almost coincides at Al end cap to crystal distance of 9 mm and after that again diverges. This indicates that the Al end cap to crystal distance should be taken as 9 mm instead of 3 mm (quoted by the manufacturer) to get a MCNP to experimental efficiency ratio independent of sample to detector distance.

But, the MCNP efficiencies were still found to be 10% higher than the experimental values at both the sample to detector distances. Further optimization was carried out to bring this factor close to unity. Previously, from Table 3, it was observed that when the detector radius is reduced by 1 mm, the efficiency ratio also reduces by about 7–9% at the two sample to detector distances. This will bring the efficiency ratio close to 1 if the optimized Al end cap to detector

crystal distance is used for MCNP calculation. Thus, the radius of the detector crystal was systematically reduced, keeping the Al end cap to crystal distance as 9 mm instead of 3 mm (given by manufacturer) and efficiency ratios at two distances were obtained. Initially, when the radius was reduced by 0.8 mm, the efficiency ratio at the two distances, $d = 1.7$ and 21.7 cm, reduced to 1.03 and 1.01, respectively (Table 5). This indicates that the ratio is approaching 1 as desired. Therefore, the radius was further reduced systematically in steps of 0.1 mm and the results are given in Table 5. When the radius is reduced by 0.9 mm, the average ratio at $d = 1.7$ and 21.7 cm was found to be close to unity, indicating that the manufacturer supplied crystal radius should be reduced by 0.9 mm to match the MCNP efficiencies with experimental efficiencies. But still at $d = 1.7$ cm, a slight systematic bias showing the dependence on energy was observed. The ratio of MCNP and experimental efficiencies were found to be higher at lower energies (1.10 at 88 keV) compared to higher energies (1.00 at 1115 keV). To remove this slight energy dependence, the dead layer thickness was increased by 0.1 mm. These calculations were done using the optimized Al end cap to crystal distance and the optimized detector crystal radius. With this variation, the

Table 5 The comparison of experimental and MCNP efficiencies at two sample to detector distances, $d = 1.7$ and 21.7 cm

Energy (MeV)	Al end cap to crystal distance, $d_{alc} = 9$ mm			
	Nominal values of all other detector parameters MCNP/exp	Crystal radius reduced by 0.8 mm MCNP/exp	Crystal radius reduced by 0.9 mm MCNP/exp	Crystal radius reduced by 0.9 mm and dead layer increased by 1 mm MCNP/exp
$d = 1.7$ cm				
0.088	1.15	1.10	1.10	1.05
0.122	1.11	1.06	1.05	1.03
0.136	1.12	1.06	1.06	1.04
0.279	1.03	0.97	0.96	0.95
0.32	1.09	0.98	0.97	0.96
0.661	1.07	1.00	0.99	0.98
1.115	1.14	1.01	1.00	0.99
Avg.	1.10	1.03	1.02	1.00
SD	0.04	0.05	0.05	0.04
% RSD	3.78	4.96	5.10	3.97
$d = 21.7$ cm				
0.088	1.08	1.01	1.00	0.97
0.122	1.10	1.03	1.02	1.00
0.136	1.09	1.01	1.00	0.99
0.279	1.08	1.00	0.99	0.98
0.32	1.05	0.97	0.96	0.96
0.661	1.12	1.03	1.01	1.01
1.115	1.10	1.00	0.99	0.98
Avg.	1.09	1.01	1.00	0.98
SD	0.02	0.02	0.02	0.02
% RSD	2.02	1.84	1.87	1.77

The MCNP efficiencies are computed by taking the optimized the Al end cap to detector crystal distance as the basis and further optimization by changing the detector radius and dead layer thickness
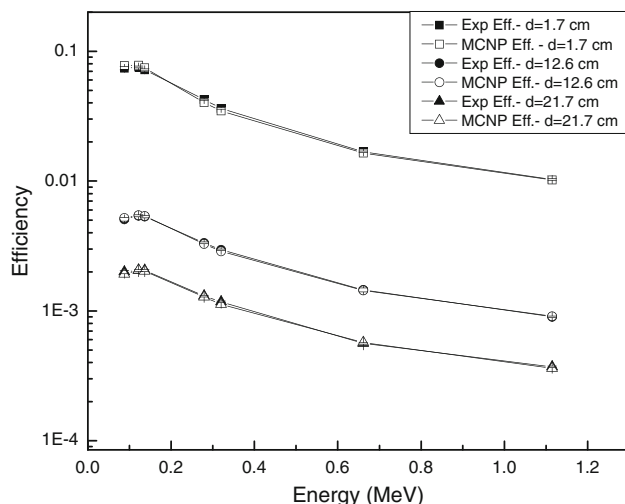
Fig. 3 Experimental and MCNP simulated FEP efficiency for point source geometry using the optimized detector geometry at three sample to detector distances, $d = 1.7$, 12.6 and 21.7 cm

Table 6 Ratios of MCNP to experimental efficiencies for 5 ml sources of ^{109}Cd, ^{57}Co, ^{203}Hg, ^{137}Cs and ^{65}Zn and for 100 ml ^{152}Eu source

Energy (MeV)	5 ml		Energy (MeV)	100 ml
	$d = 2.0$ cm	$d = 10.3$ cm		$d = 19.8$ cm
0.088	1.11	1.07	0.122	1.04
0.122	1.07	1.05	0.244	1.03
0.136	1.06	1.01	0.344	1.01
0.279	1.12	1.03	0.779	1.03
0.661	1.01	1.02	0.867	1.02
1.115	1.01	1.02	0.964	1.01
			1.112	1.04
			1.408	1.02
Avg.	1.07	1.03	Avg.	1.02
SD	0.05	0.02	SD	0.01
% RSD	4.46	2.06	% RSD	1.21

efficiency ratios were found to be within 5% at all energies and over all sample to detector distances. This experimental and the MCNP efficiencies calculated using this optimized geometry has been shown in Fig. 3. The detector parameters for the optimized geometry have been given in the last column of Table 1.

Vargas et al. [12] reported the effect of systematic variation of detector parameters on the simulated efficiencies of point and volumetric sources. The study showed significant deviations in the efficiency, depending on the source geometry and the photon energy, could be produced by varying only slightly some of the detector parameters. Of particular importance in the context of the present work, is the variation of efficiencies with the Al end cap to crystal distance for different source geometries. It has been observed [12] that this distance is critical for volumetric sources, but less important for point sources. However, our studies show that there is a strong distance dependence of simulated efficiencies with respect to experimental efficiencies for point sources also when manufacturer supplied detector parameters are used. It was also observed that this can be eliminated by adjusting the Al end cap to crystal distance.

In accordance with the principle of efficiency transfer, this optimized geometry should be valid for all the extended sample geometries. As a check of the optimized geometry, the efficiencies of 5 ml aqueous solutions of ^{109}Cd, ^{57}Co, ^{203}Hg, ^{137}Cs and ^{65}Zn in cylindrical vials at $d = 2.0$ and 10.3 cm were compared with the MCNP calculated efficiencies. The MCNP efficiencies for these samples geometries were calculated by using the optimized detector geometry and the detailed sample geometry. Table 6 gives the experimental and MCNP efficiencies along with their ratios for 5 ml sources. The two efficiencies differ by about

7% at $d = 2.0$ cm and by 3% at $d = 10.3$ cm for this extended geometry. The validity of the optimized geometry was also checked for another extended source of standard 100 ml ^{152}Eu. The experimental efficiencies at $d = 19.8$ cm for this geometry were compared with the efficiencies calculated by using MCNP. The ratios of the two efficiencies are given in the last column of the Table 6. In this case also, the two efficiencies are within 3–4%. The slight difference in the efficiencies for volumetric samples at closer distance can be due to some inaccuracy in sample geometry such as in its radius, glass thickness, its density and height. This has been also observed by Johnston et al. [6] and Vargas et al. [12] where it was observed that the sample dimensions could have a significant effect on the detector efficiency. However, our results of simulated efficiencies using adjusted detector parameters based on point source efficiencies can be used for volumetric sources also and one can get results within 5%.

Conclusion

This methodology is useful in getting an efficiency calibration not only in the cases where standards are not available but also where multi-gamma standards are available but low level counting is required.

References

1. Sima O, Arnold D (2009) On the Monte Carlo simulation of HPGe gamma-spectrometry systems. Appl Radiat Isot 67:701–705

2. Vidmar T et al (2008) An intercomparison of Monte Carlo codes used in gamma-ray spectrometry. Appl Radiat Isot 66(6–7): 764–768

3. Tzika F, Stamatelatos IE, Kalef-Ezra J, Bode P (2004) Large sample neutron activation analysis: corrections for neutron and gamma attenuation. Nukleonika 49(3):115–121

4. Ródenas J, Pascual A, Zarza I, Serradell V, Ortiz J, Ballesteros L (2003) Analysis of the influence of germanium dead layer on detector calibration simulation for environmental radioactive samples using the Monte Carlo method. Nucl Instrum Methods in Phys Res A 496:390–399

5. Nakamura T, Suzuki T (1983) Monte Carlo Calculation of peak efficiencies of Ge(Li) and pure Ge detectors to voluminal sources and comparison with environmental radioactivity measurement. Nucl Instrum Methods 205:211–218

6. Johnston PN, Hult M, Gasparro J (2006) Cascade summing effects in close geometry gamma-ray spectrometry. Appl Radiat Isot 64:1323–1328

7. Helmer RG, Hardy JC, Iacob VE, Sanchez-Vega M, Neilson RG, Nelson J (2003) The use of Monte Carlo calculations in the determination of a Ge detector efficiency curve. Nucl Instrum Methods Phys Res A 511:360–381

8. Hardy JC, Iacob VE, Sanchez-Vega M, Effinger RT, Lipnik P, Mayes VE, Willis DK, Helmer RG (2002) Precise efficiency calibration of an HPGe detector: source measurements and Monte Carlo calculations with sub-percent precision. Appl Radiat Isot 56:65–69

9. Dryak P, Kovar P (2006) Experimental and MC determination of HPGe detector efficiency in the 40–2754 keV energy range for measuring point source geometry with the source-to-detector distance of 25 cm. Appl Radiat Isot 64:1346–1349

10. Budjáš D, Heisel M, Maneschg W, Simgen H (2009) Optimisation of the MC-model of ap-type Ge-spectrometer for the purpose of efficiency determination. Appl Radiat Isot 67:706–710

11. Huy NQ, Binh DQ, An VX (2007) Study on the increase of inactive germanium layer in a high-purity germanium detector after a long time operation applying MCNP code. Nucl Instrum Methods in Phys Res A 573:384–388

12. Vargas MJ, Timón AF, Díaz NC, Sánchez DP (2002) Influence of the geometrical characteristics of an HpGe detector on its efficiency. J Radioanal Nucl Chem 253(3):439–443

13. Kamboj S, Kahn B (2003) Use of Monte Carlo simulation to examine gamma-ray interactions in germanium detectors. Radiat Meas 37:1–8

14. Liye L, Jizeng MA, Binquan Z, Yueru J (2004) Efficiency calibration of a P-Type coaxial HPGe detector with measurements and an EGS4 user code HPGe-MC. In: International radiation physics society workshop on frontier research in radiation physics and related areas, Chengdu, China Paper collection, p 204

15. Binquan Z, Jizeng MA, Jianping C, Liye L, Yong M (2005) Calculation of the detection efficiency of an HPGe detector in Low energy. Nucl Electron Detect Technology 25(3):274–277 (in Chinese)

16. Bochud F, Bailat CJ, Buchillier T, Byrde F, Schmid E, Laedermann JP (2006) Simple Monte-Carlo method to calibrate well-type HPGe detectors. Nucl Instrum Methods Phys Res A 569: 790–795

17. Tzika F, Kontogeorgakos D, Vasilopoulou T, Stamatelatos IE (2010) Application of the Monte Carlo method for the calibration of an in situ gamma spectrometer. Appl Radiat Isot 68: 1441–1444

18. Karamanis D (2003) Efficiency simulation of HPGe and Si(Li) detectors in g- and X-ray spectroscopy. Nucl Instrum Methods Phys Res A 505:282–285

19. Lepy MC et al (2001) Intercomparison of efficiency transfer software for gamma-ray spectrometry. Appl Radiat Isot 55: 493–503

20. Wang Z, Kahn B, Valentine JD (2002) Efficiency calculation and coincidence summing correction of a germanium detector by Monte-Carlo simulation. IEEE Trans Nucl Sci 49(4):1925–1931

21. Mukhopadhya PK (2001) Proceedings of symposium on intelligent nuclear instrumentation, Mumbai, p 307

22. Firestone RB (1996) Table of isotopes, 8th edn. Wiley-Interscience Publishing, New York

23. Briesmeister JF (2000) MCNP—a general Monte Carlo N-particle transport code version 4C. LA-13709-M. Los Alamos National Laboratory, Los Alamos

24. Laborie J-M, Petit GL, Abt D, Girard M (2000) Monte Carlo calculation of the efficiency calibration curve and coincidence-summing corrections in low-level gamma ray spectrometry using well-type HPGe detectors. Appl Radiat Isot 53:57–62